

# RSC Advances



This is an *Accepted Manuscript*, which has been through the Royal Society of Chemistry peer review process and has been accepted for publication.

*Accepted Manuscripts* are published online shortly after acceptance, before technical editing, formatting and proof reading. Using this free service, authors can make their results available to the community, in citable form, before we publish the edited article. This *Accepted Manuscript* will be replaced by the edited, formatted and paginated article as soon as this is available.

You can find more information about *Accepted Manuscripts* in the [Information for Authors](#).

Please note that technical editing may introduce minor changes to the text and/or graphics, which may alter content. The journal's standard [Terms & Conditions](#) and the [Ethical guidelines](#) still apply. In no event shall the Royal Society of Chemistry be held responsible for any errors or omissions in this *Accepted Manuscript* or any consequences arising from the use of any information it contains.

Cite this: DOI: 10.1039/c0xx00000x

www.rsc.org/xxxxxx

## ARTICLE TYPE

## Adsorptions of Cd(II) and Methylene Blue from Aqueous Solution by Silica Hybrid Hollow Spheres

Jing Hu,<sup>a,b</sup> Liqin Liu<sup>a</sup> and Zuobing Xiao<sup>a,b\*</sup>

Received (in XXX, XXX) Xth XXXXXXXXX 20XX, Accepted Xth XXXXXXXXX 20XX

DOI: 10.1039/b000000x

**ABSTRACT:** Silica hybrid hollow spheres were successfully synthesized by co-hydrolysis and condensation reactions of TEOS and vinyltrimethoxysilane (VTMS) under the catalysis of ammonia. The as-obtained silica hybrid hollow spheres were used as adsorbents for the removal of Cd(II) and methylene blue (MB) from aqueous solutions. The isotherm adsorption data of the silica hybrid hollow spheres for Cd(II) and MB followed the Langmuir isotherm model. The silica hybrid hollow spheres exhibited the adsorption capacities as high as 54.702 and 25.242 mg g<sup>-1</sup> for Cd(II) and MB, respectively. The adsorption kinetics of Cd(II) and MB onto the silica hybrid hollow spheres can be well fitted to the pseudo-second-order model. The adsorption processes of Cd(II) and MB onto the silica hybrid hollow spheres at 298, 318 and 338 K could be carried out spontaneously.

## Introduction

It has been known that heavy metals ions and organic dyes are main two kinds of water contaminations. For example, Cd(II) as one of the most common heavy metal ions, has become a great threat to human health.<sup>1</sup> Exposure to even low concentration of Cd(II), has potential to cause neurological, reproductive, cardiovascular and developmental disorder for human beings.<sup>2</sup> Higher level of Cd(II) exposure could increase risks of cancer mortality, and damage to liver, kidneys and bones.<sup>3,4</sup> Their non-biodegradability and biological accumulation make Cd(II) a long presence in environment and ecological chains. In addition, synthetic dyes containing difficultly decomposed aromatic structures or azo groups would be carcinogenic and mutagenic for aquatic organisms. Their discharge into water would further increase the chemical oxygen demand and decrease light penetration and visibility.<sup>5,6</sup> Although MB as a thiazine dye is not recognized as acutely hazardous, it has various harmful impacts such as nausea, vomiting and gastritis.<sup>7-9</sup>

Adsorption has been regarded as an effective and economic method for removal of pollutants in the past decades due to its easy operation process, high efficiency and low cost.<sup>10</sup> Conventional adsorbents come from nature or industrial waste such as peanut hulls,<sup>7,11</sup> rice husks,<sup>12</sup> ash,<sup>13</sup> etc.<sup>14,15</sup> However, they still exhibit many disadvantages including low adsorption capacity, fluctuant adsorption performance and limited resource. Nowadays, new types of silica based adsorbents have attracted a great deal of interest for their large specific area, controllable surface structure, and good adsorption capacity and separation.<sup>16-19</sup> For example, Ho *et al.*<sup>20</sup> fabricated ordered mesoporous adsorbents by grafting amino- and carboxylic-containing

functional groups onto MCM-41 for the removal of MB from wastewater. Pérez-Quintanilla *et al.*<sup>21</sup> prepared SBA-15 chemically modified with 2-mercaptopyrimidine using a homogeneous method and this solid was employed as Cd(II) adsorbent. Machida *et al.*<sup>22</sup> introduced mono-amino and mercapto-groups through grafting or co-condensation method onto the mesoporous silica. The functionalized mesoporous silica was proved to be an efficient adsorbent for Cd(II) (28.11 mg g<sup>-1</sup>). Alothman *et al.*<sup>23</sup> grafted mesoporous silica with di-, tri- and penta-amine functional groups and these adsorbents exhibited excellent potential for separation and preconcentration of Cu(II), Zn(II) and Cd(II). Further, Wang *et al.*<sup>24</sup> successfully functionalized SBA-15 with N-[3-(trimethoxysilyl)propyl]ethylene-diamine and used for removal of heavy metal ions in aqueous solution. Other silica materials with different structures such as silica nanofibers, gel and nanocomposites can also be used as adsorbents to remove metal ions and dyes.<sup>25,26</sup> Hollow structured silica has been also used to remove organic and inorganic pollutants owing to its large capacity, low density, thermal stability, low toxic, mild synthetic condition and easily controllable morphology.<sup>27-33</sup> Najafi *et al.*<sup>34</sup> prepared silica nano hollow spheres with rather monodisperse size through the conventional soft method. The maximum adsorption capacity of the synthesized nano particles for Cd(II) was 49.5 mg g<sup>-1</sup>. Zhang *et al.*<sup>35</sup> synthesized magnetic Fe<sub>3</sub>O<sub>4</sub>@hierarchical silica hollow spheres by microemulsification method. The spheres exhibited an excellent ability to adsorb MB from aqueous solutions with maximum adsorption capacity of 71.4 mg g<sup>-1</sup>. Recently, Zhao and Xu<sup>36</sup> fabricated 0.8 - 4 μm hollow amino-functionalized organosilica microspheres with an open hole on the shell based on the hydrolysis and condensation of 3-aminopropyltriethoxysilane and TEOS in an aqueous system without an additional template and catalyst. The adsorption capacity of this organosilica microspheres for Cd(II) was 47.4 mg g<sup>-1</sup> due to the binding between Cd(II) and the amino groups.

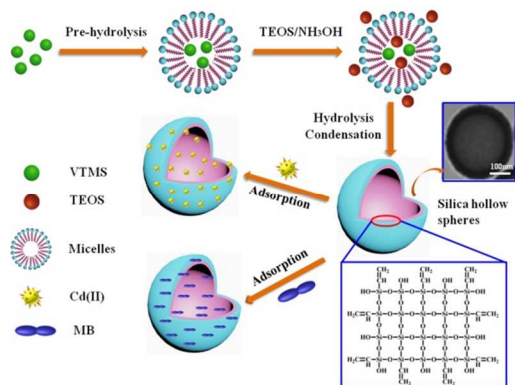
In this study, we successfully synthesize silica hybrid hollow spheres without any open holes via one simple hydrolysis and condensation of vinyltrimethoxysilane (VTMS) and

<sup>a</sup>School of Perfume and Aroma Technology, Shanghai Institute of Technology, Shanghai, 201418, China

<sup>b</sup> Shanghai Research Institute of Fragrance & Flavor Industry, Shanghai, 200232, P. R. China

\*Email: xzbsit@163.com,

tetraethoxysilane (TEOS) with ammonia as catalyst at room temperature. The as-obtained silica hybrid hollow spheres can be used as adsorbent to remove Cd(II) and MB in aqueous solution as shown in **Scheme 1**. Furthermore, the adsorption isotherm, kinetics and thermodynamic properties of the silica hybrid hollow spheres for Cd(II) and MB have been measured and discussed in details.



**Scheme 1.** Schematic diagram of the silica hybrid hollow spheres via one step and their adsorption for Cd(II) and MB

## Experimental procedure

### Materials

Vinyl trimethoxysilane (VTMS,  $\text{CH}_2\text{CHSi}(\text{OCH}_3)_3$ ,  $\geq 97\%$ ) was obtained from Evonik Specialty Chemical (Shanghai) Co., Ltd. Cadmium chloride ( $\text{CdCl}_2$ ,  $>99\%$ ), methylene blue (MB,  $\geq 94\%$ ), tetraethoxysilane (TEOS,  $\text{Si}(\text{OCH}_2\text{CH}_3)_4$ ,  $99\%$ ) and ammonia (25wt%  $\text{NH}_3$  in water) were obtained from Sinopharm Chemical Reagent Corp. All chemicals were used as received without further purification. Deionized water was used throughout the experiment.

### Synthesis of silica hybrid hollow spheres

Typically, VTMS (0.2 g) and  $\text{H}_2\text{O}$  (50 g) were charged into a 100 mL two neck round flask equipped with a mechanical stirrer, a thermometer with a temperature controller and a Graham condenser and then mechanically stirred at  $40^\circ\text{C}$  by 500 rpm for 1 h to hydrolyze VTMS. Then TEOS (1 g) and ammonia (20  $\mu\text{L}$ ) were added and stirred at the same temperature for another 3 h to produce the silica hybrid hollow spheres. The as-obtained silica hybrid hollow spheres were centrifuged and washed with absolute ethanol two times. For comparison, the silica hybrid solid spheres were also prepared with VTMS (1g) and TEOS (0.2g) according to the above process.

### Characterization

Transmission electron microscopy (TEM) images were observed with a Hitachi H-800 transmission electron microscope at 75KV. Scanning electron microscopy (SEM) images was recorded on a Philips XL 30 field emission microscope at an accelerating voltage of 10 kV. Fourier transform infrared spectra (FTIR) were obtained using a Nicolet Nexus 470 FTIR with powder-pressed KBr pellets. Raman results were determined using a LABRAM-EB raman spectroscopy. Nitrogen adsorption-desorption isotherm analysis was performed using Micromeritics

ASAP 2010. The specific surface area was characterized with the Brunauer–Emmett–Teller (BET) method. The pore size distribution was calculated from the analysis of the isotherm desorption curves using the Brunauer–Joyner–Halenda (BJH) method.

### Heavy metal ion and organic dye adsorption experiment

In order to study the adsorption capacity of the obtained silica hybrid hollow spheres, the organic and inorganic materials such as Cd(II) ions and MB were utilized. Batch adsorption experiment was performed in 100 mL-conical flasks containing 25mg adsorbents and 25mL Cd(II) ion or MB solution, shaken at 150 rpm for 12h at  $(25 \pm 1)^\circ\text{C}$ . The pH of the aqueous solution was adjusted by using either 0.1 M HCl or 0.1 M NaOH. A sample of silica hybrid hollow spheres (25 mg) was suspended in 25 mL of  $100\text{ mg L}^{-1}$  Cd (II) ions solution at several pH values (2, 3, 4, 5, 6, 7). This is because that Cd (II) would precipitate from the solution when pH is  $>7$ . But pH of MB solution was chosen from 2 to 10 at the concentration of  $30\text{ mg L}^{-1}$  MB. Adsorption isotherms were carried out with the varying initial concentrations of Cd(II) ions (10, 20, 40, 60, 80, 100, 150, 200, 300, 400, 500  $\text{mg L}^{-1}$ ) at pH 4 and those of MB (5, 10, 15, 20, 25, 30, 35, 40, 60, 80, 100  $\text{mg L}^{-1}$ ) at pH 8. To study the effect of time, the adsorption time of Cd(II) ions was controlled from 0 to 300 min at the initial concentrations of  $100\text{ mg L}^{-1}$  and pH 4. That of MB was chosen from 0 to 420 min at the initial concentrations of  $30\text{ mg L}^{-1}$  and pH 8. These kinetic experiments were performed by using the batch technique. After an aliquot of Cd(II)/MB solution at the predetermined time intervals was removed, the remain solution didn't continue to use. Then, the next determination should be obtained by using a new solution with the same concentration. Adsorption thermodynamics was conducted at the temperatures ranging from 298K to 338 K with varying initial concentration of Cd(II) (100, 150, 200, 300, 400,  $500\text{ mg L}^{-1}$ ) and MB (10, 15, 20, 25, 30,  $35\text{ mg L}^{-1}$ ) for 12h.

After a desired adsorption period, the silica hybrid hollow spheres were separated from the solution, and then the concentration of Cd(II) ions was measured by the atomic absorption spectrophotometry using a AA 240 DUO instrument. That of MB was determined by UV/Vis Spectrometer (UV 2100). The adsorption capacity of the adsorbates (Cd(II) ion and MB) at equilibrium was calculated according to the following equation:<sup>37</sup>

$$q_e = \frac{(c_0 - c_e)v}{m} \quad (1)$$

where  $q_e$  is the equilibrium adsorption capacity of adsorbent ( $\text{mg of metal g}^{-1}$  adsorbent),  $C_0$  is the initial concentration of adsorbate in  $\text{mg L}^{-1}$ ,  $C_e$  is the equilibrium concentration of adsorbate in  $\text{mg L}^{-1}$ ,  $v$  is the volume of the adsorption medium in L, and  $m$  is the weight of the adsorbent in g. All the experiments were carried out in triplicate and their mean value was reported.

## Results and discussions

### Preparation of silica hybrid hollow spheres

**Fig. 1** displays the typical TEM and SEM images of silica hybrid hollow spheres and solid spheres. Monodisperse silica hybrid hollow spheres have the average size of 390 nm with a shell thickness of 50 nm as shown in Fig.1a, and their surfaces

are little bit rough (Fig. 1 b). When more VTMS was used, solid spheres with the mean size of 1.2 $\mu$ m are obtained (Fig. 1c and 1d).

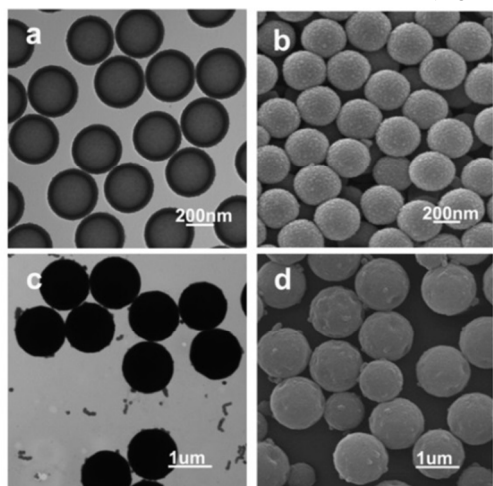


**Fig. 1** Typical TEM and SEM images of silica hybrid hollow spheres (a, b) and silica hybrid solid spheres (c, d)

The FTIR spectra of silica hybrid hollow spheres, silica hybrid solid spheres and SiO<sub>2</sub> particles are illustrated in **Fig. 2**. The strong absorption bands at 1100 cm<sup>-1</sup> and 470 cm<sup>-1</sup> are assigned to the stretching vibration of Si-O-Si groups. The broad and strong peak at 3420 cm<sup>-1</sup> is attributed to Si-OH stretching vibration. Except these characteristic peaks of SiO<sub>2</sub> particles, the spectra of the silica hybrid hollow spheres and solid spheres exhibit the absorption bands at 3062 cm<sup>-1</sup>, 2961 cm<sup>-1</sup> attributing to the vibration absorptions of -CH and CH<sub>2</sub>= groups, respectively. The strong peak at 1602 cm<sup>-1</sup> is related to the vibration of C=C groups, while the bands at 1407 cm<sup>-1</sup> and 1278 cm<sup>-1</sup> are for the bending banding deformations of Si-CH=CH<sub>2</sub> groups and the rocking vibrations of -CH<sub>2</sub>= groups. This identifies the existence of vinyl groups in these hybrid spheres. Furthermore, in the spectrum of the silica hybrid solid spheres, the peaks associated with C=C, CH<sub>2</sub>= and -CH<sub>2</sub>= groups are enhanced with increasing the amount of VTMS obviously. This demonstrates that the organic vinyl groups have been linked on Si-O-Si chains of these hollow spheres.

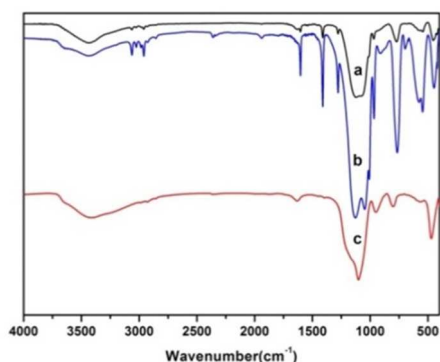


**Fig. 2** FTIR spectrum of silica hybrid hollow spheres (a), silica hybrid solid spheres (b) and SiO<sub>2</sub> particles (c)

The existence of vinyl groups on the silica hybrid spheres can be further verified by Raman (**Fig. 3**). For silica hybrid hollow and solid spheres, the stretching modes of C=C groups are observed at 1604 cm<sup>-1</sup>, while the scissoring and rocking vibration of CH<sub>2</sub>= and -CH<sub>2</sub>= groups occur at 1415 and 1276 cm<sup>-1</sup>,

respectively. For silica hybrid solid spheres, the stronger peaks associated with C=C, CH<sub>2</sub>= and -CH<sub>2</sub>= groups are observed, indicating higher grafting density with the increasing amount of VTMS.

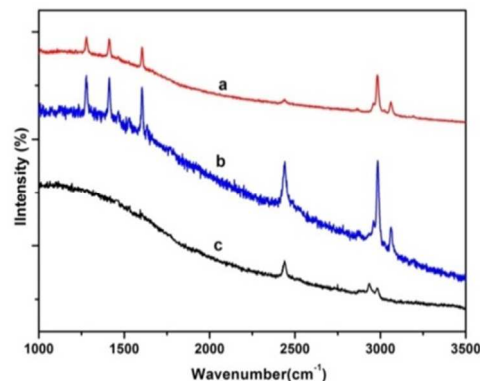


**Fig. 3** Raman spectrum of silica hybrid hollow spheres (a), silica hybrid solid spheres (b) and SiO<sub>2</sub> particles (c)

**Fig. 4** shows the typical nitrogen adsorption/desorption isotherms and pore size distribution of silica hybrid hollow spheres and solid spheres. The N<sub>2</sub> adsorption-desorption isotherms of the silica hybrid hollow spheres exhibit the representative type-IV curves. The BET surface area, pore volume and mean pore size of the silica hybrid hollow spheres are 259.9 m<sup>2</sup> g<sup>-1</sup>, 0.36 cm<sup>3</sup> g<sup>-1</sup> and 4.25 nm due to their special hollow structures, which are significantly larger than those of the solid hybrid spheres (52.4 m<sup>2</sup> g<sup>-1</sup>, 0.23 cm<sup>3</sup> g<sup>-1</sup> and 1.60 nm, respectively).

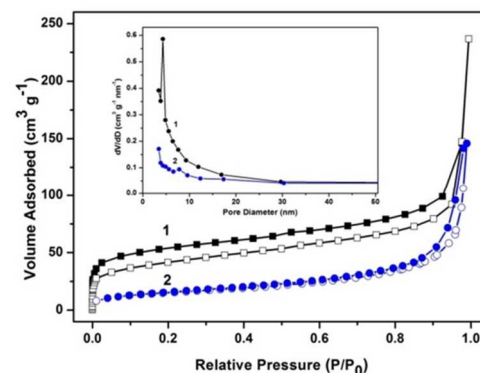


**Fig. 4** Nitrogen adsorption/desorption isotherms of silica hybrid hollow spheres (1) and silica hybrid solid sphere (2). Inset: distribution of pore size.

## Adsorption properties

### Effect of pH

pH is one of the most important parameters governing the remove of metal ions and dye from the aqueous solution by adsorption.



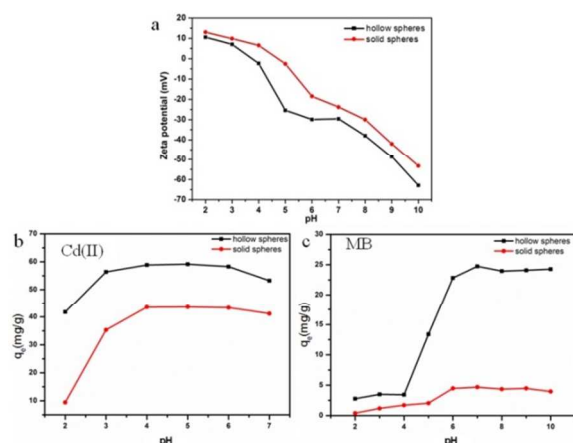


**Fig. 5** The effect of pH on zeta potentials (a) and the adsorption capacity of Cd(II) (b) and MB(c) onto silica hybrid hollow spheres and solid spheres

**Fig. 5** demonstrates the effect of pH on Cd(II) and MB adsorption by silica hybrid hollow spheres and solid spheres. For both Cd(II) and MB, the silica hybrid hollow spheres still have obviously much higher adsorption capacity than the solid spheres, because the former has larger BET surface area and more –OH groups. The isoelectric points (pI) of silica hybrid hollow spheres and solid spheres are 3.8 and 4.7, respectively (Fig. 5a). The adsorption of Cd(II) by the silica hybrid spheres increases with pH increasing from 2.0 to 4.0, and reaches the equilibrium with pH from 4.0 to 6.0, then decreased with pH increasing from 6.0 to 7.0. This is due to the fact that both the spheres exhibit positive charges and would reject with Cd (II) at pH < pI. When pH > 5, both the spheres remain negatively charged. The adsorption capacity decreases sharply with increasing of pH from 4.0 to 7.0, this is likely attributed to that the pores of spheres are filled up with Cd(OH)<sub>2</sub> precipitation from the hydroxylated complexes of the Cd(II). Therefore, the optimum pH 4.0 for Cd (II) is chosen throughout the subsequent experiment. Fig. 5 c demonstrates that the MB adsorption capacity of both silica hybrid hollow spheres and solid spheres is growing slowly at pH < pI due to the electrostatic repulsion between MB and the excessive H<sup>+</sup> ions on their surface. Then the adsorption of MB by the silica hybrid hollow spheres increases quickly at pH > pI and get the equilibrium with pH from 8 to 10. The negatively charged Si-OH groups on the surfaces of the silica hybrid spheres favor the adsorption of cationic dye molecules. However, the solid spheres exhibit little adsorption capacity for MB as shown in Fig. 5c (0.395 mg g<sup>-1</sup> – 5.211 mg g<sup>-1</sup>). This implies that MB is only absorbed on the surface of the solid spheres via electrostatic interaction due to their small BET surface area, pore volume and pore size (52.4 m<sup>2</sup> g<sup>-1</sup>, 0.23 cm<sup>3</sup> g<sup>-1</sup> and 1.60 nm).

### Adsorption isotherms

Langmuir and Freundlich mathematic models were used to

**Table 1** Langmuir and Freundlich isotherm constants for Cd(II) and MB onto silica hybrid hollow spheres and solid spheres.

Adsorbate	Sorbent	Langmuir model			Freundlich model		
		$q_m$ (mg/g)	$b$	$R^2$	$k$	$n$	$R^2$
Cd(II)	Hollow spheres	54.702 ± 2.174	0.037 ± 0.006	0.9692	11.726 ± 2.074	3.889 ± 0.053	0.9256
	Solid spheres	48.401 ± 5.090	0.013 ± 0.004	0.9865	3.798 ± 1.716	2.496 ± 0.053	0.8259
MB	Hollow spheres	25.242 ± 0.875	0.679 ± 0.117	0.9817	12.937 ± 1.666	5.865 ± 0.143	0.8944
	Solid spheres	5.811 ± 0.246	0.342 ± 0.095	0.9875	2.981 ± 0.338	6.379 ± 0.132	0.9126

explain the adsorption isotherms. A Langmuir adsorption model assumes the monolayer coverage of adsorbent surface with homogeneous binding sites. The Langmuir equation is given by Eq.(2).<sup>38</sup>

$$q_e = \frac{q_m b C_e}{1 + b C_e} \quad (2)$$

Where  $C_e$  and  $q_e$  are equilibrium adsorbate concentration (mg L<sup>-1</sup>) and equilibrium adsorption capacity (mg g<sup>-1</sup>).  $q_m$  (mg g<sup>-1</sup>) is the maximum uptake capacity corresponding to complete monolayer coverage and  $b$  (L g<sup>-1</sup>) is Langmuir constant that represents the affinity between solute and adsorbent.

A Freundlich isotherm is based on the assumption of the heterogeneous adsorption due to the diversity of the adsorption sites or the diverse nature of the metal ions adsorbed. The Freundlich equation is expressed as Eq.(3):<sup>39</sup>

$$q_e = k C_e^{\frac{1}{n}} \quad (3)$$

Where  $k$  and  $n$  are the Freundlich constants, related to the adsorption capacity of adsorbent and adsorption intensity, respectively.

**Fig. 6** illustrates the typical adsorption isotherms of silica hybrid hollow spheres and solid spheres as a function of different adsorbates (Cd(II) and MB ) concentrations. The fitting results for the adsorption of Cd(II) and MB on silica hybrid hollow spheres and solid spheres are calculated and listed in **Table 1**. The Langmuir model is much better than the Freundlich model, suggesting that the adsorption of Cd(II) and MB by silica hybrid hollow spheres and solid spheres is homogenous. The values of  $q_m$  are found to be 54.702 and 48.401 mg g<sup>-1</sup> for Cd(II), and 25.242 and 5.811 mg g<sup>-1</sup> for MB on the silica hybrid hollow spheres and solid spheres, respectively. Obviously, the silica hybrid hollow spheres exhibit the superior adsorption property due to their special hollow structures and more –OH groups. The BET surface area, pore volume and mean pore size of the silica hybrid hollow spheres (259.9 m<sup>2</sup> g<sup>-1</sup>, 0.36 cm<sup>3</sup> g<sup>-1</sup> and 4.25 nm) are larger than those of the solid hybrid spheres (52.4 m<sup>2</sup> g<sup>-1</sup>, 0.23 cm<sup>3</sup> g<sup>-1</sup> and 1.60 nm). The capillary force between the inside and outside of the silica hybrid hollow spheres is a primary one causing migrations of Cd(II) and MB. Meanwhile, the MB adsorption capacity of the solid spheres is lowest due to its only surface adsorption. The average pore size calculated from BJH method for the solid spheres is 1.60 nm, which is too small to stop the MB molecules with 1.43 nm length × 0.61 nm width × 0.4 nm height penetrating inside the spheres<sup>40</sup>. While the average diameter of Cd (II) is 0.095 nm [Taken from Ionic radius table], which allow itself to migrate towards the inside of the spheres.

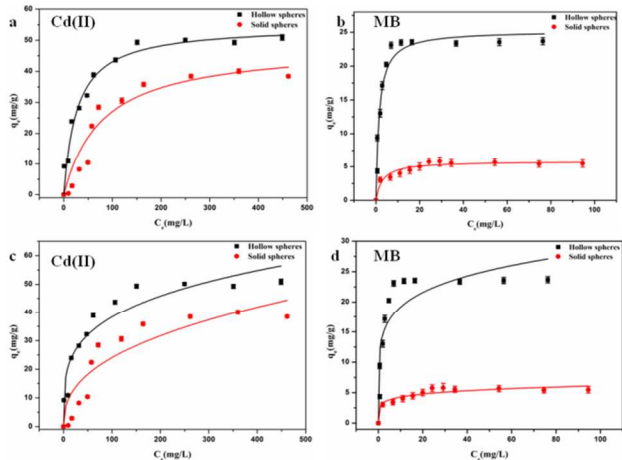


**Fig. 6** The adsorption isotherms with Langmuir (a and b) and Freundlich (c and d) on silica hybrid hollow spheres and solid spheres.

### Adsorption kinetics

The kinetics of adsorption that describes the adsorbents uptake rate governing the contact time of the adsorption reaction is one of the important characteristics that define the efficiency of adsorption. In this study, the kinetics of the adsorption process was studied by batch experiments at room temperature. A sample of 25 mg of the silica hybrid hollow spheres and solid spheres was used in each experiment, and the initial concentrations of Cd(II) and MB were 100 mg·L<sup>-1</sup> and 30 mg·L<sup>-1</sup>, respectively. **Fig.7a** shows the adsorption kinetic curves of the silica hybrid hollow spheres and solid spheres as the example to Cd(II) and MB. It can be seen that the MB adsorption by the silica hybrid hollow spheres reaches the equilibrium within initial 5 min quickly. However, this adsorption by the silica hybrid solid spheres is very rapid in the first 25min, and then slows down in the following time, and finally reaches the equilibrium after 60 min. On the contrary, the Cd(II) adsorption onto both the silica hybrid hollow spheres and solid spheres increases sharply in the first 50 min and then reaches the equilibrium (Fig. 7b).

The adsorption kinetic data of Cd(II) and MB onto both the spheres are analyzed in terms of pseudosecond-order kinetic equations. This equation is based on the assumption that the determining rate step would be chemisorption promoted by

covalent forces through the electron exchange, or valency forces through electrons sharing between adsorbent and adsorbate. The liner form of the pseudo-second-order model is expressed as Eq.(4, 5):<sup>41-43</sup>

$$\frac{t}{q_t} = \frac{t}{q_e} + \frac{1}{k_2 q_e^2} \quad (4)$$

$$h_0 = k_2 q_e^2 \quad (5)$$

Where  $q_t$  is the amount of adsorbate at any time (mg g<sup>-1</sup>),  $q_e$  is the amount of adsorbate at equilibrium (mg g<sup>-1</sup>);  $K_2$  is the adsorption constant (min<sup>-1</sup>),  $h_0$  is the initial adsorption rate (g mg<sup>-1</sup> min<sup>-1</sup>).

The fitting curve of pseudo-second-order kinetic model and the corresponding kinetic parameters are illustrated in Fig.7(c, d) and **Table 2**. The determination coefficients ( $R^2$ ) of the silica hybrid hollow spheres and solid spheres are 0.9927 and 0.9875 for Cd(II) adsorption, and 0.9991 and 0.9964 for MB, respectively. The theoretical  $q_e$  value ( $q_{e, cal}$ ) estimated from the pseudo-second-order kinetic model is close to the experimental values of  $q_e$  ( $q_{e, exp}$ ). These results suggest that the whole process controlling the rate may be a chemical adsorption.

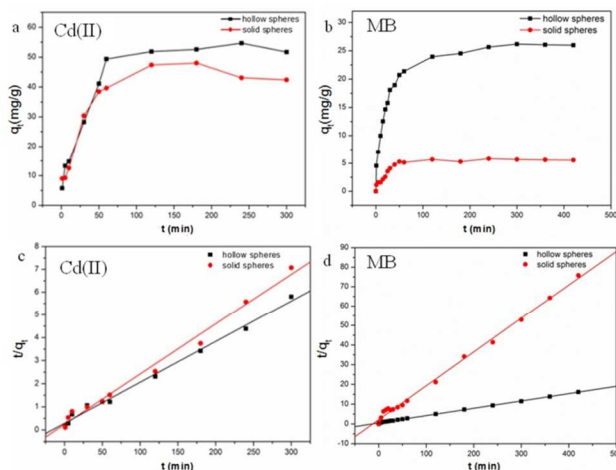


**Fig. 7** Effect of adsorption time on the adsorption behavior (a, b) and Pseudo-second-order kinetic model fitting (c, d) of silica hybrid hollow spheres and solid spheres.

**Table 2** Pseudo-second-order model constants for Cd(II) and MB adsorption on silica hybrid hollow spheres and solid spheres

Adsorbate	Sorbent	$q_{e,exp}$ (mg/g)	Pseudo-second-order			
			$q_{e,cal}$ (mg/g)	$h_0$ (g·mg <sup>-1</sup> ·min <sup>-1</sup> )	$K_2$ (min <sup>-1</sup> )	$R^2$
Cd(II)	Hollow spheres	52.712±1.267	55.788±0.022	3.945±0.027	0.0013±<0.0001	0.9927
	Solid spheres	45.213±2.885	45.589±0.073	4.752±0.029	0.0023±<0.0001	0.9875
MB	Hollow spheres	25.203±2.124	27.333±0.016	1.881±0.023	0.0025±<0.0001	0.9991
	Solid spheres	5.386±0.038	5.523±0.063	0.435±0.012	0.014±0.0007	0.9964

### Thermodynamic Studies

The thermodynamic parameters provide in-depth information about the energetic changes associated with adsorption process. Thermodynamic parameters, such as change in enthalpy ( $\Delta H^\theta$ ), entropy ( $\Delta S^\theta$ ) and Gibbs free energy ( $\Delta G^\theta$ ) can be determined by the following Eq.(6, 7):<sup>44,45</sup>

$$\Delta G^\theta = -RT \ln K_c \quad (6)$$

$$\ln K_c = \frac{\Delta S^\theta}{R} - \frac{\Delta H^\theta}{RT} \quad (7)$$

where  $R$  is the universal gas constant (8.314 J mol<sup>-1</sup> K<sup>-1</sup>),  $T$  (K) is the absolute temperature,  $K_c$  is the thermodynamic equilibrium constant.  $K_c$  is obtained by plotting  $\ln(q_e/C_e)$  versus  $q_e$  and extrapolating to zero as shown in Fig. S1. Table 3 displays the values of  $\ln K_c$ . The values of  $\Delta H^\theta$  (KJ mol<sup>-1</sup>) and  $\Delta S^\theta$  (J mol<sup>-1</sup> K<sup>-1</sup>) can be further obtained from the slop and interception of the van't

Hoff linear plots of  $\ln K_c$  versus  $1/T$  by using Eq.(7) (Fig.8). The change of adsorption Gibbs free energy ( $\Delta G^\theta$ ) can be calculated from Eq. (6).

**Table 3** summarizes all the thermodynamic parameters. The positive values of  $\Delta H^\theta$  indicate that the adsorption process of Cd(II) and MB onto the silica hybrid hollow spheres and the solid spheres is endothermic. The positive  $\Delta S^\theta$  indicates an irregular increase of the randomness at the adsorbent/solution interface during the adsorption procedure. The negative values of  $\Delta G^\theta$  by the silica hybrid hollow sphere obtained at all of the experimental temperatures display that the adsorption process could be carried out spontaneously. As the temperature increases, the value of  $\Delta G^\theta$  decreases. This indicates that the adsorption is more favorable in high temperature. However, the positive values of  $\Delta G^\theta$  for MB onto the solid sphere indicate that the adsorption between solid spheres and MB molecules is not spontaneous.

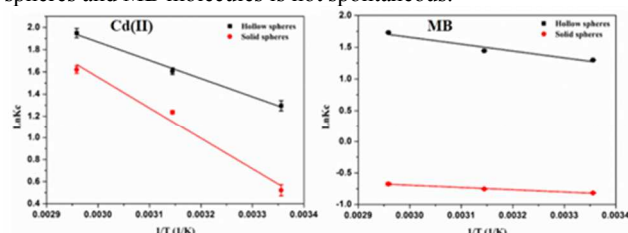


**Fig. 8** Plots of  $\ln K_c$  versus  $1/T$  for adsorption of Cd(II) and MB on silica hybrid hollow spheres and solid spheres

## Conclusion

**Table 3** Thermodynamic parameters for Cd(II) and MB adsorption on silica hybrid hollow spheres and solid spheres

Adsorbate	Sorbent	Temperature (K)	$\ln K_c$	$\Delta G^\theta$ (J mol <sup>-1</sup> )	$\Delta S^\theta$ (J mol <sup>-1</sup> K <sup>-1</sup> )	$\Delta H^\theta$ (kJ mol <sup>-1</sup> )	$R^2$
Cd(II)	Hollow spheres	298	1.295	-3208.393 ± 11.135			
		318	1.572	-4156.912 ± 76.661	56.319 ± 1.087	12.665 ± 0.042	0.9665
		338	1.949	-5477.327 ± 11.816			
	Solid spheres	298	0.522	-1292.507 ± 28.727			
		318	1.253	-3313.284 ± 41.664	84.211 ± 1.063	23.812 ± 0.041	0.9594
		338	1.596	-4485.369 ± 94.601			
MB	Hollow spheres	298	1.297	-3213.731 ± 27.706			
		318	1.445	-3819.541 ± 19.342	40.769 ± 0.321	8.999 ± 0.012	0.9067
		338	1.730	-4862.796 ± 15.698			
	Solid spheres	298	-0.818	2027.846 ± 12.724			
		318	-0.755	1997.283 ± 12.424	3.626 ± 0.754	3.118 ± 0.021	0.9650
		338	-0.675	1898.099 ± 47.209			

## References

- M. Waseem, S. Mustafa, A. Naeem, K.H. Shah and I. Shah, *Chem. Eng. J.*, 2011, **169**, 78.
- H. N. Kim, W. X. Ren, J. S. Kim and J. Y. Yoon, *Chem. Soc. Rev.*, 2012, **41**, 3210.
- C. N. McFarland, L. I. Bendell-Young, C. Guglielmo and T. D. Williams, *J. Environ. Monitor.*, 2002, **4**, 791.
- D. Li and Y. N. Xia, *Nano. Lett.*, 2003, **3**, 555.
- S. Y. Mak and D. H. Chen, *Dyes Pigments*, 2004, **61**, 93.
- L. L. Fan, Y. Zhang, X. J. Li, C. N. Luo, F. G. Lu and H. M. Qiu, *Colloid. Surface. B.*, 2012, **91**, 250.
- D. Özer, G. Dursun and A. Özer, *J. Hazard. Mater.*, 2007, **144**, 171.
- A. Özer and G. Dursun, *J. Hazard. Mater.*, 2007, **146**, 262.
- L. M. Cui, Y. G. Wang, L. H. Hu, L. Gao, B. Du and Q. Wei, *RSC Adv.*, 2015, **5**, 9759.
- L. Liu, Y. R. Zhang, Y. J. He, Y. F. Xie, L. H. Huang, S. Z. Tan and X. Cai, *RSC Adv.*, 2015, **5**, 3965.
- P. Brown, I. A. Jefcoat, D. Parrish, S. Gill and E. Graham, *Adv. Environ. Res.*, 2000, **4**, 19.
- V. Vadivelan and K. V. Kumar, *J. Colloid. Interf. Sci.*, 2005, **286**, 90.
- M. Rafatullah, O. Sulaiman, R. Hashim and A. Ahmad, *J. Hazard. Mater.*, 2010, **177**, 70.
- B. H. Hameed, *J. Hazard. Mater.*, 2009, **162**, 344.
- I. A. W. Tan, A. L. Ahmad and B. H. Hameed, *J. Hazard. Mater.*, 2009, **164**, 473.
- K. F. Lam, K. L. Yeung and G. McKay, *Environ. Sci. Technol.*, 2007, **41**, 3329.
- Y. H. Wu, M. L. Zhang, H. Y. Zhao, S. X. Yang and A. Arkin, *RSC Adv.*, 2014, **4**, 61256.

- 18 E. Petala, K. Dimos, A. Douvalis, T. Bakas, J. Tucek, R. Zbořil and M. A. Karakassides, *J. Hazard. Mater.*, 2013, **261**, 295.
- 19 L. Sun, S. C. Hu, H. M. Sun, H. L. Guo, H. D. Zhu, M. X. Liu and H. H. Sun, *RSC Adv.*, 2015, **5**, 11837.
- 20 K. Y. Ho, G. McKay and K. L. Yeung, *Langmuir*, 2003, **19**, 3019.
- 21 D. Pérez-Quintanilla, I. D. Hierro, M. Fajardo and I. Sierra, *J. Mater. Chem.*, 2006, **16**, 1757.
- 22 M. Machida, B. Fotoohi, Y. Amamo, T. Ohba, H. Kanoh and L. Mercier, *J. Hazard. Mater.*, 2012, **221–222**, 220.
- 23 Z. A. Allothman and A. W. Apblett, *J. Hazard. Mater.*, 2010, **182**, 581.
- 24 Z. Q. Wang, M. Wang, G. H. Wu, D. Y. Wu and A. G. Wu, *Dalton Trans.*, 2014, **43**, 8461.
- 25 Z. J. Ma, H. J. Ji, Y. Teng, G. P. Dong, J. J. Zhou, D. Z. Tan and J. R. Qiu, *J. Colloid. Interf. Sci.*, 2011, **358**, 547.
- 26 P. Yin, Q. Xu, R. J. Qu, G. F. Zhao and Y. Z. Sun, *J. Hazard. Mater.*, 2010, **173**, 710.
- 27 M. Chen, L. M. Wu, S. X. Zhou and B. You, *Adv. Mater.*, 2006, **18**, 801.
- 28 J. Hu, M. Chen, X. S. Fang and L. M. Wu, *Chem. Soc. Rev.*, 2011, **40**, 5472.
- 29 S. Hyuk Im, U. Jeong and Y. N. Xia, *Nat. Mater.*, 2005, **4**, 671.
- 30 F. Q. Tang, L. L. Li and D. Chen, *Adv. Mater.*, 2012, **24**, 1504.
- 31 S. S. Cao, L. Fang, Z. Y. Zhao, Y. Ge, S. Piletsky and A. P. F. Turner, *Adv. Funct. Mater.*, 2013, **23**, 2162.
- 32 Z. X. Wang, L. M. Wu, M. Chen and S. X. Zhou, *J. Am. Chem. Soc.*, 2009, **131**, 11276.
- 33 J. Hu, X. G. Wang, L. Q. Liu and L. M. Wu, *J. Mater. Chem. A.*, 2014, **2**, 19771.
- 34 M. Najafi, Y. Yousefi and A. A. Rafati, *Sep. Purif. Technol.*, 2012, **85**, 193.
- 35 J. X. Zhang, B. S. Li, W. L. Yang and J. J. Liu, *Ind. Eng. Chem. Res.*, 2014, **53**, 10629.
- 36 X. L. Yang, N. Zhao, Q. Z. Zhou, Z. Wang, C. T. Duan, C. Cai, X. L. Zhang and J. Xu, *J. Mater. Chem.*, 2012, **22**, 18010.
- 37 J. Chung, J. Y. Chun, J. Lee, S. H. Lee, Y. J. Lee and S. W. Hong, *J. Hazard. Mater.*, 2012, **239–240**, 183.
- 38 X. B. Luo, L. L. Liu, F. Deng and S. L. Luo, *J. Mater. Chem. A*, 2013, **1**, 8280.
- 39 M. B. Jazi, M. Arshadi, M. J. Amiri and A. Gil, *J. Colloid. Interf. Sci.*, 2014, **422**, 16–24.
- 40 C. Pelekani and V. L. Snoeyink, *Carbon*, 2000, **38**, 1423.
- 41 B. X. Liu, J. S. Wang, J. S. Wu, H. Y. Li, Z. F. Li, M. L. Zhou and T. Y. Zuo, *J. Mater. Chem. A*, 2014, **2**, 1947.
- 42 W. L. Sun, J. Xia and Y. C. Shan, *Chem. Eng. J.*, 2014, **250**, 119.
- 43 A. Heidari, H. Younesi and Z. Mehraban, *Chem. Eng. J.*, 2009, **153**, 70.
- 44 S. Mustafa, M. Waseem, A. Naeem, K. H. Shah and T. Ahmad, *Desalination*, 2010, **255**, 148.
- 45 G. Annadurai, L. Y. Ling and J. F. Lee, *J. Hazard. Mater.*, 2008, **152**, 337.





RSC Advances Accepted Manuscript